Published in final edited form as:
Sci Transl Med. 2012 March 21; 4(126): 126ra34. doi:10.1126/scitranslmed.3003122.

Prostaglandin D_2 Inhibits Hair Growth and Is Elevated in Bald Scalp of Men with Androgenetic Alopecia

Luis A. Garza[1,*], **Yaping Liu**[2], **Zaixin Yang**[1], **Brinda Alagesan**[1], **John A. Lawson**[3], **Scott M. Norberg**[1], **Dorothy E. Loy**[4], **Tailun Zhao**[1], **Hanz B. Blatt**[1], **David C. Stanton**[5], **Lee Carrasco**[5], **Gurpreet Ahluwalia**[6,†], **Susan M. Fischer**[7], **Garret A. FitzGerald**[3], and **George Cotsarelis**[1,‡]

[1]Department of Dermatology, Kligman Laboratories, University of Pennsylvania School of Medicine, Philadelphia, PA 19104, USA

[2]Screening and Protein Sciences, Merck & Company, North Wales, PA 19454, USA

[3]Department of Pharmacology and the Institute for Translational Medicine and Therapeutics, University of Pennsylvania School of Medicine, Philadelphia, PA 19104, USA

[4]Department of Dermatology, Johns Hopkins University School of Medicine, Baltimore, MD 21231, USA

[5]Department of Oral and Maxillofacial Surgery, University of Pennsylvania School of Medicine, Philadelphia, PA 19104, USA

[6]Gillette Corporation, Foxborough, MA 02035, USA

[7]University of Texas M. D. Anderson Cancer Center, Science Park–Research Division, Smithville, TX 78957, USA

Abstract

Testosterone is necessary for the development of male pattern baldness, known as androgenetic alopecia (AGA); yet, the mechanisms for decreased hair growth in this disorder are unclear. We show that prostaglandin D_2 synthase (PTGDS) is elevated at the mRNA and protein levels in bald scalp compared to haired scalp of men with AGA. The product of PTGDS enzyme activity, prostaglandin D_2 (PGD_2), is similarly elevated in bald scalp. During normal follicle cycling in mice, *Ptgds* and PGD_2 levels increase immediately preceding the regression phase, suggesting an inhibitory effect on hair growth. We show that PGD_2 inhibits hair growth in explanted human hair follicles and when applied topically to mice. Hair growth inhibition requires the PGD_2 receptor G

‡To whom correspondence should be addressed. cotsarel@mail.med.upenn.edu.
*Present address: Department of Dermatology, Johns Hopkins University School of Medicine, Baltimore, MD 21231, USA.
†Present address: Allergan Inc., Irvine, CA 92623, USA.

SUPPLEMENTARY MATERIALS
www.sciencetranslationalmedicine.org/cgi/content/full/4/126/126ra34/DC1

Author contributions: L.A.G. and G.C. designed the studies, analyzed and interpreted the results, and co-wrote the paper. Y.L. and Z.Y. performed the microarrays. L.A.G. and G.C. selected PTGDS for further analysis. L.A.G. performed reverse transcription–PCR, ELISA, Western blotting, lipid extractions, histology, and mouse work, with assistance from B.A., S.M.N., T.Z., H.B.B., and D.E.L. J.A.L. performed mass spectrometry and interpretations. G.A.F. supervised mass spectrometry and aided with interpretations and design. D.C.S. and L.C. provided expertise in male pattern baldness and discarded tissue samples. A.G. performed and supervised human hair-lengthening experiments. S.M.F. provided the K14-*Ptgs2* mice and assisted with interpretation and design.

Competing interests: A.G. is an inventor of a patent owned by the Gillette Corporation to use PGD_2 to inhibit hair growth. L.A.G. and G.C. are co-inventors of a patent owned by the University of Pennsylvania describing the PGD_2 pathway as a target for inhibiting hair loss, among other claims. The Pennsylvania Department of Health specifically disclaims responsibility for any analyses, interpretations, or conclusions.

Data and materials availability: The K14-*Ptgs2* mouse is under materials transfer agreement from the University of Texas M. D. Anderson Cancer Center.

protein (heterotrimeric guanine nucleotide)–coupled receptor 44 (GPR44), but not the PGD_2 receptor 1 (PTGDR). Furthermore, we find that a transgenic mouse, K14-*Ptgs2*, which targets *prostaglandin-endoperoxide synthase 2* expression to the skin, demonstrates elevated levels of PGD_2 in the skin and develops alopecia, follicular miniaturization, and sebaceous gland hyperplasia, which are all hallmarks of human AGA. These results define PGD_2 as an inhibitor of hair growth in AGA and suggest the PGD_2-GPR44 pathway as a potential target for treatment.

INTRODUCTION

Eighty percent of Caucasian men experience some degree of androgenetic alopecia (AGA) before age 70 (1). Testosterone is necessary for AGA to develop, and a genetic susceptibility locus in the androgen receptor is present in a minority of men with AGA; however, additional factors contributing to this disorder remain unknown (2–4). Studies on AGA have the potential to yield insights into other androgen-mediated diseases, such as benign prostatic hypertrophy and prostate cancer (5). Current legitimate treatments for AGA include finasteride, minoxidil, and hair transplantation (6). Finasteride inhibits 5-α reductase 2 (SRD5A2), which converts testosterone to a more potent androgen, dihydrotestosterone. Although the active targets of minoxidil in AGA therapy are not known, suggested ones include potassium channels or prostaglandins. Specific examples of the latter have not been conclusively identified (7).

In AGA, large “terminal” hair follicles forming thick hair shafts miniaturize over time to small follicles that generate microscopic effete hairs (8). Follicle miniaturization is accompanied by a decrease in the duration of the growing phase of the follicle (anagen), which normally lasts several years to produce hair more than 1 m long, but which decreases to only days or weeks in AGA. This results in an increase in the percentage of resting (telogen) hair follicles containing microscopic hairs in bald scalp (4). In addition to these intrinsic changes to the hair follicle, infiltrating lymphocytes and mast cells have been identified around the miniaturizing follicle (9), especially in the area of the stem cell–rich bulge area (10). Sebaceous glands, which attach to each follicle, hypertrophy in bald scalp (8). In balding scalp, the number of hair follicle stem cells remains intact, whereas the number of more actively proliferating progenitor cells markedly decreases (11). This suggests that balding scalp either lacks an activator or has an inhibitor of hair follicle growth.

Here, we used a global gene expression approach to define differentially expressed genes in balding versus nonbalding scalp from the same individuals. We found elevated levels of prostaglandin D_2 synthase (PTGDS) at the message and protein levels in balding versus haired scalp from men with AGA. Given the described metabolism of prostaglandins in the human hair follicle (12, 13), we focused on the synthase, both in mouse (Ptgds) and in human (PTGDS). The enzymatic product of PTGDS, prostaglandin D_2 (PGD_2), was also elevated in bald human scalp tissue. We show a close temporal relationship between elevations in both *Ptgds* mRNA and PGD_2 levels in mice with hair follicle regression during normal hair follicle cycling. We further provide functional data indicating that PGD_2 and its nonenzymatic metabolite, 15-deoxy-Δ12,14-prostaglandin J_2 (15-$dPGJ_2$), inhibit hair growth in both mouse and human hair follicles. In mice and humans, the PGD_2-mediated inhibition of hair growth required the G protein (heterotrimeric guanine nucleotide–binding protein)–coupled receptor 44 (GPR44), but not the prostaglandin D_2 receptor 1 (PTGDR). Finally, we describe a mouse model (K14-*Ptgs2*) with elevated PGD_2 levels in the skin that phenocopies human AGA (14). These results implicate PGD_2 in the pathogenesis of AGA and suggest new receptor targets for its treatment.

RESULTS

PTGDS and PGD_2 are elevated in bald scalp

To assess global gene expression changes in the bald scalp of men with AGA, we performed gene expression microarrays comparing bald to haired scalp in five men with AGA. Correlation coefficients among haired and among bald replicate samples approached 1 (Fig. 1A). Correlation coefficients comparing haired to bald scalp within individuals were also close to 1, indicating the advantage of paired samples as internal controls.

We identified 250 transcripts that were differentially expressed in human haired versus bald scalp. As evidence for the validity of these transcripts, a clustering algorithm sorted out samples as either haired or bald, on the basis of the expression of these genes (Fig. 1B). Hair keratins were up-regulated in haired scalp, as would be expected. For unclear reasons, hemoglobin-related transcripts were elevated in bald scalp. In haired scalp, 169 genes were elevated, and 81 genes were elevated in bald scalp, with the expected directions of expression (Fig. 1C). We determined enriched gene ontology functional classifications for these genes and identified overlapping categories. In the haired scalp, morphogenesis and developmental pathway genes were overexpressed, whereas in the bald scalp immune response genes were overexpressed (Fig. 1D), consistent with the known histology of AGA (9).

Considering the clinical use of prostaglandin $F_{2\alpha}$ ($PGF_{2\alpha}$)–related compounds to promote hair growth (15), and the often antagonistic functions of prostaglandins (16), we were intrigued to find *PTGDS* as one of the most highly expressed transcripts in human male balding scalp (Fig. 1, E and F). Of the three probe sets that covered *PTGDS* on the microarray, all were elevated in balding scalp (Fig. 1E). Increased *PTGDS* expression and PTGDS protein levels were further confirmed in balding versus haired human scalp by real-time quantitative polymerase chain reaction (qPCR) (Fig. 2A) and Western blotting (Fig. 2, B and C).

To better understand the role of PTGDS in balding, we measured levels of its synthase product, PGD_2, in both balding and haired human scalps. We discovered a significant increase in PGD_2 in the balding scalp compared to haired scalp by immunoassay (Fig. 2D). The absolute level of PGD_2 was 16.3 ng/g tissue in balding scalp and 1.5 ng/g tissue in haired scalp. PGD_2 levels were then measured using ultra–high-performance liquid chromatography–mass spectrometry (UHPLC-MS) because of its reported superior accuracy in measuring prostaglandins compared to immunoassay (17). In a larger series of paired bald and haired samples from 17 men with AGA, we noted an increase in PGD_2 in bald scalp compared to haired scalp (Fig. 2E).

Other prostaglandins have activity on hair follicle growth. We measured levels of additional prostaglandin species in balding and haired scalps. The nonenzymatic metabolite of PGD_2, 15-$dPGJ_2$, was also increased in balding scalp compared to haired scalp (Fig. 2E). However, the absolute level of 15-$dPGJ_2$ (3.8 ng/g bald scalp, 1.3 ng/g haired scalp) was lower than PGD_2 (53.5 ng/g bald scalp, 25.6 ng/g haired scalp) (Fig. 2F). UHPLC-MS did detect higher levels of PGD_2 in balding scalp than immunoassay (53.5 versus 16.3 ng/g tissue), although both methods demonstrated increased PGD_2 mass in bald scalp. In contrast to PGD_2, the level of prostaglandin E_2 (PGE_2), which is synthesized by PTGES rather than PTGDS, was more abundant in haired scalp compared to balding scalp (Fig. 2E), with 3.1 ng/g balding scalp and 6.4 ng/g haired scalp as detected by UHPLC-MS (Fig. 2F).

Nonpermanent follicle mouse keratinocytes express Ptgds at the end of anagen

To better understand the normal biological function of Ptgds and PGD_2 on hair growth, we capitalized on the well-characterized, synchronized hair cycle of the mouse (18). Fluctuations in gene expression and protein levels can be tracked to different stages of the hair follicle cycle by examining skin at different ages or after depilation of the mouse hair, which induces a synchronized new hair follicle cycle. In the process of investigating the features of the synchronized mouse hair cycle, we verified hair cycle stage relative to postnatal (PN) day in mouse skin biopsy samples. We confirmed that, as suggested by gross appearance, the histological features of mice at PN21 were those of late telogen, PN35 of late anagen, and PN46 of catagen (fig. S1).

Ptgds mRNA, as measured by qPCR, peaked in the late stage of anagen and was sevenfold higher compared to the resting phase (telogen) at PN20 (Fig. 3A). Thus, *Ptgds* expression was lowest during telogen and increased progressively through anagen to peak at late anagen near the time of transition to catagen, the phase of regression. To more closely examine the proximity of the *Ptgds* expression peak to the catagen transition, we compared it to the expression of *fibroblast growth factor 5* (*Fg f5*), a known marker of catagen onset (19). *Fg f5* expression peaked in late anagen compared to telogen (Fig. 3A). Together, *Fg f5* and *Ptgds* peak expression levels overlapped during late anagen, just before the onset of catagen.

We next sought to identify control genes expressed differently from *Fg f5* and *Ptgds*. As a marker of early anagen, we measured the expression of the receptor for $PGF_{2\alpha}$, which is known for its ability to induce hair growth both in mice (20) and in humans (15). In contrast to the late peak of *Ptgds* and *Fgf5*, prostaglandin F receptor (*Ptgfr*) mRNA peaked in early anagen or late telogen, with a 21-fold change versus second telogen (PN52) (Fig. 3A) and a 3-fold change versus first telogen (PN20).

To determine the temporal relationship between expression of *Ptgds* and the production of PGD_2, we measured PGD_2 levels by HPLC-MS in identical mice from which mRNA data were determined in Fig. 3A. We discovered that PGD_2 production peaked after the apex of *Ptgds* expression. During the catagen stage, at PN46, PGD_2 reached a peak level of 87.6 ng/g tissue compared to a nadir in early anagen on PN24 of 7.4 ng/g tissue (Fig. 3B). Thus, *Ptgds* mRNA is first expressed in the skin in late anagen, and subsequently, PGD_2 is produced via Ptgds protein during catagen.

Although early hair follicle cycle stages in individual mice are naturally synchronized, animals of the same age and even litter can exhibit heterogeneity with respect to hair follicle cycling. Therefore, we repeated the above analysis using mice that had been depilated simultaneously to synchronize the hair cycle between animals as well as within animals. Corroborating our results from the spontaneous hair cycle, *Ptgds* mRNA also fluctuated with the hair cycle in depilated animals. *Ptgds* mRNA peaked in late anagen, followed by the peak of PGD_2 in catagen (Fig. 3C). PGD_2 production peaked on day 19.5 (catagen), with 199.9 ng/g tissue compared to a nadir of 27.6 ng/g tissue on day 37. We also noted a unique peak of PGD_2 production within hours of depilation, which was not seen in the spontaneous hair cycle in Fig. 3B. This coincides with degranulation of mast cells observed previously after depilation (21). The more narrow peaks of markers in the depilated hair cycle likely reflect tighter synchronization of the hair follicle cycle after depilation. To better define expression of Ptgds, we performed immunohistochemistry on tissue sections from skin of the animals used for the time course in Fig. 3C. Ptgds was evident in late anagen in the keratinocytes of the outer root sheath below the stem cell–rich bulge area marked by the arrector pili muscle (Fig. 3D) (10). This area of the follicle regresses during catagen.

To corroborate this pattern seen by immunohistochemistry, we next examined double immunofluorescence labeling for both Ptgds and keratin 15 (Krt15), a hair follicle stem cell marker (22). At day 0 of depilation (telogen), Krt15 was present in the bulge area at the most inferior permanent part of the hair follicle, which persists into telogen (Fig. 3E). We did not identify Ptgds, which was consistent with qPCR data showing lack of expression of *Ptgds* during telogen (Fig. 3A). Also consistent with qPCR, at day 17 (late anagen), we found a detectable *Ptgds* pattern by immunostaining (Fig. 3, D and F). Lower outer root sheath cells —but not bulge cells—expressed Ptgds. Furthermore, at day 19 after depilation, keratinocytes in catagen follicles expressed Ptgds, without overlapping Krt15-positive keratinocytes (Fig. 3G). These results demonstrate that Ptgds is abundant in nonpermanent keratinocytes of the hair follicle in mouse.

PTGDS is expressed in nonpermanent keratinocytes of the human hair follicle

In normal terminal human hair follicles, we found a similar presence of PTGDS, primarily in the nonpermanent hair follicle below the arrector pili muscle (Fig. 4A). However, staining was variable with many normal human follicles exhibiting little or no staining (Fig. 4B). This is consistent with lower levels of *PTGDS* mRNA in haired versus bald scalp and likely also reflects the lack of synchronicity in human hair follicle cycling. In miniaturized hair follicles in balding human scalp, sebaceous gland and hair follicle keratinocytes outside of the bulge (Fig. 4, C and E), and in some cases within the suprabasal bulge (Fig. 4D), expressed PTGDS. We also detected PTGDS outside of the hair follicle epithelium, indicating potential sources of PGD_2 in the dermis (Fig. 4, E and F). In hair follicles undergoing catagen, PTGDS was present in mast cells within the fibrous streamer, which is the former site of the regressed follicle (Fig. 4E). These results in mouse and human demonstrate that the lipocalin PTGDS and its product PGD_2 are predominantly expressed in the transient portion of the follicle at a time when the follicle begins regressing. These findings are in line with our hypothesis that the PGD_2 pathway inhibits hair follicle growth.

Transgenic mice overexpressing *Ptgs2* in the epidermis phenocopy AGA

Given the correlation of increased levels of PGD_2 with balding scalp in humans and the presumptive inhibitory role of PGD_2 on the mouse follicle, we hypothesized that mice with high levels of PGD_2 in the skin might develop features of AGA. Because Ptgs2 (cyclooxygenase 2, prostaglandin G/H synthase) is the enzyme upstream to Ptgds, we further hypothesized that mice overexpressing *Ptgs2* would have elevated PGD_2 levels. Transgenic mice that overexpress *Ptgs2* in the epidermis had been developed previously for carcinogenesis studies. The hair follicles in these K14-*Ptgs2* transgenic mice were noted to enter catagen prematurely, and these mice reportedly developed alopecia and sebaceous gland enlargement (14, 23).

We further analyzed the skin and hair follicles of the K14-*Ptgs2* mouse. These mice developed alopecia, which was evident as a decrease in the normal murine pelage coat compared to control (Fig. 5, A and B). By histology, we also detected sebaceous gland hyperplasia as indicated by enlarged sebocytes clustered around the hair follicle (Fig. 5, C and D). The hair follicles in the K14-*Ptgs2* mice were miniaturized compared to controls (Fig. 5, C and D), and these follicles bore a marked resemblance to the miniaturized follicles in human bald scalp.

To determine the prostaglandin content in the alopecic skin of the K14-*Ptgs2* mice, we measured prostaglandin levels by HPLC-MS during the anagen phase of the hair follicle cycle. PGE_2 was elevated in the K14-*Ptgs2* mice compared to age-matched wild-type controls, as was previously shown using immunoassays measuring PGE_2 and $PGF_{2\alpha}$ content in biopsied mouse skin (14, 24). PGD_2 was also elevated and was more abundant than PGE_2

in both wild-type and K14-*Ptgs2* mice. 15-dPGJ$_2$ was elevated in K14-*Ptgs2* mice compared to controls and demonstrated the largest fold increase (~14-fold), although baseline values were low (5.7 ng/g tissue) (Fig. 5E). We found low levels (18.4 ng/g tissue) of PGF$_{2\alpha}$, and an absence of prostacyclin (6k-PGF$_{1\alpha}$) and thromboxane (TxB$_2$) (Fig. 5E), which are not known to be present in normal skin. Together, the balding phenotype in these mice is likely a result of the overwhelming PGD$_2$ and 15-dPGJ$_2$ inhibitory effects on the hair follicle, despite the presence of PGE$_2$, a known promoter of hair growth (20).

15-dPGJ$_2$ and PGD$_2$ inhibit hair growth in mouse and human hair follicles

Given the temporal peak of PGD$_2$ before the apoptotic catagen stage, the published ability of its metabolite 15-dPGJ$_2$ to induce apoptosis in other cell types, we tested the effects of the prostaglandins on primary cell culture of keratinocytes isolated from neonatal foreskin. 15-dPGJ$_2$ induces apoptosis (fig. S2A), as evidenced by plasma membrane blebbing and cell retraction/shrinkage. 15-dPGJ$_2$ also decreased cell density, cell division, and live-cell numbers (fig. S2, B to D). Perhaps because the origin of these keratinocytes was not the hair follicle, PGD$_2$ had no such effect on the cells. However, 15-dPGJ$_2$ did increase sub-G$_1$ DNA quantities and activated caspase 3 in human keratinocytes, which are features of apoptotic cell death (fig. S2, E to G). We therefore hypothesized that at least 15-dPGJ$_2$, if not also PGD$_2$, could directly inhibit hair growth in vivo.

15-dPGJ$_2$ was applied topically to dorsal back skin of C57BL/6 mice that had been depilated to synchronize the hair follicle cycle. Starting on day 8 after depilation and continuing every other day, we applied 10 μg of 15-dPGJ$_2$ or acetone vehicle. Hair length was measured on days 4, 12, 14, and 16 after depilation. On days 12 to 16, hair at the site of treatment was shorter than in vehicle-treated animals (Fig. 6A). To determine a minimal effective dose, we tested the application of 1 μg of both PGD$_2$ and 15-dPGJ$_2$ as above and measured hair length on day 20 after depilation. PGD$_2$ inhibited hair growth, but to a lesser extent than 15-dPGJ$_2$ (Fig. 6B). We found no evidence of changes in hair follicle cycling grossly or by histologic examination.

Having demonstrated PGD$_2$-mediated inhibition of hair growth, we next sought to determine which receptor was responsible for this effect. The two canonical receptors for PGD$_2$ are PTGDR (also known as DP-1) and GPR44 (DP-2). Both DP-1 and DP-2 have been reported to be expressed by outer root sheath keratinocytes in the hair follicle, among other sites (12). We therefore tested the capacity for PGD$_2$ to inhibit hair growth in both *Ptgdr* null mice (25) and *Gpr44* null mice (26) using *Ptgds* null mice (27) as a control. Whereas *Ptgds* and *Ptgdr* knockout mice were both susceptible to the inhibition of hair lengthening, *Gpr44* null mice were resistant to the inhibitory effect of PGD$_2$ (Fig. 6C). These data suggest that GPR44, rather than PTGDR, is the receptor for PGD$_2$-mediated inhibition of hair lengthening and could therefore be a therapeutic target for AGA.

To test the effect of PGD$_2$ on human hair growth, we used explanted human hair follicles maintained in culture for 7 days. We added increasing amounts (from 0 to 10 μM) of PGD$_2$, 15-dPGJ$_2$, or vehicle to the culture medium and measured hair length (Fig. 6D). Starting at 5 μM, PGD$_2$ and 15-dPGJ$_2$ significantly inhibited hair growth. At 10 μM, PGD$_2$-treated hair was 62 ± 5% shorter than vehicle, whereas 10 μM 15-dPGJ$_2$ completely inhibited all hair growth. We tested a variety of other PGD$_2$ analogs and found them to be capable of inhibiting hair lengthening. Agonism for GPR44 correlated with the ability to inhibit hair lengthening (fig. S3). For example, the weak agonist 11-deoxy-11-methylene PGD$_2$ (28) had the lowest activity (hair growth inhibition) of the compounds tested. Note that GPR44 has nanomolar affinities for ligands, but as is typical for this type of experiment, higher concentrations were required to overcome tissue penetration and compound lysis. Thus, in

both mouse and human, PGD_2 and 15-$dPGJ_2$ inhibit hair growth, likely through the GPR44 receptor.

DISCUSSION

Recent evidence has illustrated a role for prostaglandins in regulating hair growth. For example, the $PGF_{2\alpha}$ analog latanoprost is Food and Drug Administration (FDA)–approved and routinely used clinically to enhance hair growth of human eyelashes (15). PGE_2 has been proposed to protect from radiation-induced hair loss in mice (29), and both PGE_2 and $PGF_{2\alpha}$ have been shown to enhance hair growth in mice (20). Our studies show that prostaglandins are dysregulated in AGA, the most common type of hair loss in men. Specifically, PGD_2 inhibits hair growth and thus represents a negative counterbalance to the positive effects on hair growth shown for PGE_2 and $PGF_{2\alpha}$.

There is precedence for the opposing functions of individual prostaglandins that are downstream from the PTGS enzymes. For example, in the lung, PGE_2 causes relaxation, whereas PGD_2 causes contraction of bronchial muscle tone (16). Our results suggest that in mouse and human skin, a balance between PGE_2 and PGD_2 controls hair growth. This model predicts then that efforts to reverse alopecia should optimally focus on both enhancing PGE_2 and inhibiting PGD_2 signaling. This model also explains why agents such as aspirin, which inhibit upstream prostaglandin synthesis enzymes (PTGS1 and PTGS2), have minimal effects on hair growth because of likely equally decreased production of PGE_2 and PGD_2.

Given our current report that PGD_2 inhibits hair growth, prostaglandins represent an underappreciated network for controlling the rate of hair lengthening. Evidence to support the PGD_2 pathway's direct induction of the apoptotic catagen stage includes the temporal expression of *Ptgds* with catagen onset, in vitro studies of 15-$dPGJ_2$ showing inhibition of hair growth, and the *Ptgs2*-overexpressing mouse model, which develops alopecia (23). These results are consistent with the notion that PTGDS elevation in balding scalp leads to increased levels of PGD_2 and 15-$dPGJ_2$, which then promote the onset of catagen and decrease hair lengthening, leading to the increase in telogen follicles and miniaturization of the hair follicle characteristic of AGA. PGD_2 may also cause sebaceous hyperplasia seen in AGA.

Although we did not elicit premature catagen in mice treated topically with PGD_2, we observed a negative effect on hair growth (Fig. 6). This could be explained because of inappropriate prostaglandin delivery, frequency, or concentration. Other explanations include potential cofactors that are required with PGD_2 to more directly affect hair cycling. Nevertheless, our results do suggest that prostaglandins directly modulate speed of hair growth during anagen. Current explanations of the differences in hair length by species focus mostly on duration of hair follicle cycling rather than accompanying potential differences in hair-lengthening rates during anagen (4). Our results suggest that greater attention should be paid to the possibility that prostaglandins modulate hair growth speed and that compounds increasing hair growth speed may benefit patients with AGA.

Intriguingly, *Ptgds* is a highly testosterone-responsive transcript (30, 31), which further suggests its importance in AGA. PGD_2 is thought to play a central role in male gonadal sex determination (32) and is highly expressed in male genitalia (32, 33). Similarly, *Ptgds* expression in the heart is regulated by estrogen (34). Estrogen leads to increases in 15-$dPGJ_2$ levels in the uropygial gland (35). Recent evidence also suggests that prostaglandins induce virilization of the mouse brain through estrogen (36). Given the androgens are aromatized into estrogens, these results may be relevant to hair growth and alopecia in both men and

women. Thus, these or similar pathways might be conserved in the skin and suggest that sex hormone regulation of *Ptgds* may contribute to the pathogenesis of AGA.

Additional evidence that prostaglandins control hair follicle cycling and can be used therapeutically to treat AGA arises from findings on the possible mechanism of the AGA drug minoxidil. Although minoxidil alters potassium channel kinetics (7), it is also known to increase production of PGE_2 (37). Given the decreased amount of PGE_2 present in bald scalp versus haired scalp (Fig. 2E), minoxidil may normalize PGE_2 levels. Future studies should address whether minoxidil can concomitantly decrease PGD_2 levels and thus normalize multiple prostaglandin species as a mechanism to improve AGA.

The lower absolute amount of 15-$dPGJ_2$ compared to PGE_2 and PGD_2 is particularly relevant; although this eicosanoid has been hypothesized to be a natural ligand for the nuclear hormone transcription factor peroxisome proliferators–activated receptor γ (PPARγ), the measured concentration of 15-$dPGJ_2$ is often lower than the binding constant for PPARγ (17). Thus, although it is attractive to speculate that the sebaceous gland hypertrophy and elevated levels of 15-$dPGJ_2$ observed in both human AGA and mouse K14-*Ptgds* model might be related, the causal connection is unclear. Despite this, a growing literature correlates elevated 15-$dPGJ_2$ levels with sebaceous hyperplasia, such as in acne (38). Given the common requirement of circulating sex hormones and common histology of sebaceous hyperplasia, acne and AGA may have overlapping pathogeneses.

Another report has linked altered lipid metabolism and alopecia (39). In a distinct type of human alopecia called lichen planopilaris, expression of PPARγ is decreased with accompanying altered lipid metabolism. These were discovered through an approach similar to ours using micro-array analysis of affected and unaffected scalp. The most up-regulated transcript from affected subjects, cytochrome P450 family 1 member A1 (CYP1A1), was up-regulated 1020-fold. The authors hypothesized that a xenobiotic, such as dioxin, might up-regulate CYP1A1 expression and trigger lichen planopilaris. However, cytochrome P450s also have roles in eicosanoid biology, and they may alter prostaglandin metabolism (40). Thus, altered prostaglandin metabolism might contribute to more than one type of human alopecia, although additional studies are needed.

Our findings should lead directly to new treatments for the most common cause of hair loss in men, AGA. Given its suspected role in allergic diseases, at least 10 antagonists of the GPR44 (DP-2) receptor have been identified (41) and several are in clinical trials (42). The potential for developing these compounds into topical formulations for treating AGA should elicit great interest moving forward. The question of whether similar changes in PGD_2 levels are found in the affected scalp of women with AGA also needs to be addressed. AGA in women may not be androgen-mediated, but if prostaglandins represent a final common pathway, targeting prostaglandins should benefit women with AGA as well.

Our findings also suggest that supplemental PGE_2 could be therapeutic. By correcting its deficiency and increasing its level in bald scalp, the inhibitory effects of PGD_2 may be overcome. Analogs of $PGF_{2\alpha}$, which are already FDA-approved to promote eyelash growth, should also have similar effects on the scalp and are currently in clinical trials for this indication. Once issues of delivery, dosing, and safety are addressed, additional agonists and antagonists of prostaglandin pathways should become available. The K14-*Ptgs2* transgenic mouse model, which phenocopies AGA, may assist in screening novel therapeutic agents. Ultimately, multiple mechanisms may be responsible for hair loss in AGA. Inhibiting PGD_2 may prevent miniaturization and provide benefit to those in the process of balding; however, it is unclear whether men who are already bald will regrow hair.

MATERIALS AND METHODS

Human tissue samples

This study used only normally discarded human scalp obtained anonymously and was approved by Penn's Institutional Review Board office as an exempt protocol. Normally discarded human scalp was obtained during hair transplantation as previously described (11). Tissues originated from adult Caucasian males age 40 to 65 who were not taking finasteride or minoxidil. All analyses used unique scalp samples not used in other experiments. To calculate average fold differences between haired and bald scalp, we created ratios for each patient and then averaged them. Microarrays were performed with published methods (11). Specifically, Affymetrix HG-U133A chip was used. Colors of lines and cells in graphics indicate intensity relative to that gene's median expression across all samples. For hair-lengthening experiments, discarded tissue from face lifts, which contain terminal hair, was used.

Animals

All animal protocols were approved by the University of Pennsylvania Institutional Animal Care and Use Committee. Wild-type C57BL/6J female mice were purchased from Jackson Laboratory under request for mice of identical weights and birth dates for time-course studies. K14-*Cox2* transgenic mice (14) and *Ptgdr* (25), *Gpr44* (26), and *Ptgds* (27) knockout mice were obtained from original sources. To decrease effects of endogenous testosterone, we used only female mice. Depilation to synchronize the hair cycle was performed as described (21). If an animal was found to be in a transitional state on the day of biopsy, the later-stage sample was labeled to be 12 hours more advanced.

Real-time qPCR

Mouse dorsal back skin was removed with scissors and forceps. Human tissue was cut with scissors. Tissue (25 to 35 mg) was solubilized in 300 μl of Qiagen RLT buffer. Human scalp and mouse tissues were homogenized with a tissue rotor, and RNA was collected and converted to complementary DNA (cDNA) per the manufacturer's instructions with the Fibrous RNA Extraction Kit (Qiagen) and the High-Capacity cDNA kit (Applied Biosystems). cDNA (50 ng) was used in real-time qPCRs with Fast Mix Quantitative RT-PCR Master Mix and measurements on the Step One Plus System (Applied Biosystems). β-*Actin* and 18*S* RNA probe standards were found to be equivalent to one another and did not fluctuate between samples of equal loading amounts. Fold change was calculated with the $\Delta\Delta C_T$ method. Primers used were inventoried TaqMan primers (Applied Biosystems): *PTGDS* (human), *Ptgds* (mouse), *Fgf5* (mouse), *Ptgfr* (mouse), β-*actin* (human), β-*actin* (mouse), and 18*S* (human and mouse).

Western blot

Human scalp tissue was homogenized, and protein amount was quantitated with a BCA kit (Pierce). Equal amounts for each discarded tissue lysate (15 to 35 μg) were loaded for SDS–polyacrylamide gel electrophoresis. Polyvinylidene difluoride blots were probed with mouse monoclonal anti-PTGDS (Cayman Chemical), followed by anti-mouse secondary antibody conjugated to HRP (Vector). The blot was developed with electrochemiluminescence (Amersham), exposed to autoradiography, and quantified with ImageJ (National Institutes of Health), all per the manufacturers' instructions. Blots were subsequently stained with Ponceau Red (Sigma) to verify equal loading between all lanes tested.

PGD_2 enzyme-linked immunosorbent assay

Human scalp was obtained from hair transplants to measure the amount of PGD_2. Immediately after surgery, samples were placed at 4°C in Dulbecco's modified Eagle's medium with 10% fetal bovine serum (FBS) and antibiotics/antimycotics, or they were snap-frozen. Tissue sample weights varied from 0.14 to 0.94 g. All values were normalized to the starting tissue weight. Within 1 to 2 days, samples were flash-frozen in liquid nitrogen and stored at −70°C for at least 24 hours. After thawing, samples were diluted in 1 ml of acetone and homogenized. Samples were centrifuged at 5000*g* for 10 min, supernatant was removed, and a second extraction was performed on the pellet. The combined supernatants were dried in a SpeedVac centrifuge and resuspended in 100 μl of enzyme immunoassay buffer provided in the Cayman Chemical Prostaglandin D_2-MOX ELISA (enzyme-linked immunosorbent assay) kit. Manufacturer's instructions were followed for determination of PGD_2 concentration relative to a standard curve. Values were normalized to haired scalp.

Ultra–high-performance liquid chromatography

Human tissue was prepared as above for ELISA. To maximize prostaglandin yield in mice, we snap-froze the samples and kept them below 4°C at all times. Tissue from K14-*Ptgs2* mice and Friend virus B-type (FVB) strain-matched animal controls was obtained at day 24 of life. For mouse tissues, excised epidermis and dermis were snap-frozen in acetone, minced, and homogenized with an Omni TH 115V with metal tip in acetone for less than 2 min. Homogenized tissue was then centrifuged at 16,000*g* for 10 min, with the supernatant saved. The acetone was dried under a gentle stream of nitrogen gas, after which the sample was redissolved in 1 ml of 5% acetonitrile in water, acidified with 20 μl of formic acid, and applied to a conditioned Strata-X SPE cartridge (Phenomenex). The SPE protocol included preconditioning with 1 ml of H_2O followed by 1 ml of acetonitrile, sample application, washing with 1 ml of H_2O, drying by application of house vacuum for 15 min, and elution with 1 ml of 10% acetonitrile in ethyl acetate. The eluate was then dried with a stream of nitrogen, redissolved in 200 μl of 30% acetonitrile in H_2O, and filtered through 0.2-μm Nylon Spin-X filters (Corning) before 100 μl was injected into the instrument for UHPLC analysis.

The UHPLC consisted of an Accela solvent-delivery system (Thermo) and Hypersil GOLD C18, 200 mm × 1 mm, 1.9-μm particle-size columns (Thermo). The mobile phase consisted of water (solvent A) and acetonitrile/methanol (95:5, solvent B), both with 0.005% acetic acid adjusted to pH 5.7 using ammonium hydroxide. The mobile phase gradient started at 20% B and increased in a linear manner to 35% at 10 min, followed by a linear increase to 80% B at 20 min, and held at 80% B for 3 min. The flow rate was 350 μl/min.

Mass spectrometry

A TSQ Quantum Ultra instrument (Thermo) equipped with a heated electrospray ionization (ESI) source and triple quadrupole analyzer was used. The ESI source used nitrogen for sheath and auxiliary gas, set to 70 and 5 arbitrary units, respectively. The mass spectrometer was operated in the negative ion mode with a capillary temperature of 350°C and a spray voltage of 0 kV. The source offset was set to 6 V. The analyzer was operated in the selected reaction monitoring mode. The transitions monitored for the first 16 min were as follows: mass/charge ratio (*m/z*) 351→271 (collision energy, 15 V) for endogenous PGD_2 and PGE_2, *m/z* 355→275 (15 V) for tetradeuterated PGD_2 and PGE_2, *m/z* 353→193 (24 V) for endogenous $PGF_{2\alpha}$, and *m/z* 357→197 (24 V) for tetradeuterated $PGF_{2\alpha}$. For the last 7 min, *m/z* 315→271 (15 V) for endogenous 15-dPGJ$_2$ and *m/z* 319→275 (15 V) for the tetradeuterated analog were monitored. All eicosanoids were purchased from Cayman Chemical.

Immunohistology and immunofluorescence

Mouse-back or human-scalp skin was fixed in 4% paraformaldehyde, embedded in parafilm, and sectioned at 5 to 10 μm. Non-immunoslides were stained for hematoxylin and eosin (Fisher Scientific). For immunostaining, polyclonal rabbit anti-PTGDS (Cayman Chemical) or monoclonal mouse anti-KRT15 (Lab Vision, clone LHKRT15) was applied followed by biotinylated anti-rabbit or anti-mouse, respectively. ABC kit (Vector labs) was used with horseradish peroxidase and diazoaminobenzene for color development. Methyl green (Vector Labs) was used to counterstain the tissue for immunohistochemistry; antigen staining appears brown and counterstain appears bluish green. Staining was visualized in a traditional light microscope (Nikon).

Skin was treated with the same primary antibodies as described for immunohistochemistry. Anti-rabbit Alexa Fluor 488 (Invitrogen) and anti-mouse rhodamine (Vector Labs) were used as secondary antibodies. Tissues were subsequently mounted in 4′,6-diamidino-2-phenylindole (DAPI) medium (Vector Labs). Staining was visualized in a traditional fluorescence microscope with red, green, and blue filter cubes (Leica).

Keratinocyte cell culture

Human foreskin keratinocytes were isolated from neonatal foreskins, as described previously (43). Equal densities of keratinocytes were plated (50,000 cells/cm^2) between passages 2 and 3 after initiation into six-well culture dishes. Cells were maintained in 2 ml of EpiLife medium (Cascade Biologics) and treated for 12 to 48 hours with stocks of PGD_2, PGE_2, or 15-$dPGJ_2$ (Cayman Chemical) that had been dissolved in acetone. Unless specified otherwise, cells were treated with 10 μM prostaglandins for 20 hours. Acetone alone was used as a control.

Flow cytometry

During culture, human keratinocytes were pulsed with 0.2 mM bromodeoxyuridine (BrdU) for the final 3 hours of incubation with prostaglandins. Cells were typsinized to release cells into suspension, counted, fixed, and permeabilized (Caltech). Cells were stained with 20 μl of anti–activated caspase 3 (Becton Dickinson, clone CPP32) or anti-BrdU fluorescein isothiocyanate (Becton Dickinson, clone B44) per 10^6 cells. Cells were resuspended in phosphate-buffered saline (PBS) with 5% FBS and DAPI (5 μg/ml) before being run on an LSRII flow cytometer (Becton Dickinson). Sub-G_1 cells were gated as those containing less than diploid amounts of DNA.

Mouse hair-lengthening studies

To compare the effect of vehicle, PGD_2, and 15-$dPGJ_2$ on the hair cycle among wild-type and knockout mice, we applied 1 μg of the listed prostaglandin in 200 μl of acetone or acetone alone to the central back on days 8, 10, 12, 14, 16, and 18 after depilation, with measurement of hair length performed on day 20. However, to test the time course of hair lengthening on 15-$dPGJ_2$ versus vehicle, we used 10 μg instead. Hair length was measured as described (44), with the selection of only awl (non-zigzag) hairs measured. For testing mutant mouse strains, the experiment was repeated on three separate litters.

Human hair follicle culture

The hair follicle organ culture model was performed as described (45). Briefly, human hair follicles in growth phase (anagen) were isolated from face and brow-lift tissue obtained from plastic surgeons. At least three different human donors (a mixture of men and women) were used for each compound tested. All subjects were in the age range of 40 to 60 years. The skin was sliced into thin strips of 1 to 2 mm, exposing two to three rows of follicles that

could readily be dissected. Follicles were placed into 0.5 ml of William's E medium (Life Technologies) supplemented with L-glutamine (2 mM), insulin (10 μg/ml), hydrocortisone (10 ng/ml), penicillin (100 U), streptomycin (0.1 mg/ml), and amphotericin B (0.25 μg/ml). The follicles were incubated in 24-well plates (one follicle per well) at 37°C in an atmosphere of 5% CO_2 and 95% air. PGD_2, PGD_2 metabolites, and PGD_2 analogs (Cayman Chemical) were dissolved into dimethyl sulfoxide (DMSO) as 100× stock solutions (for example, 0.5 mM for 5 μM treatments and 1 mM for 10 μM treatments). DMSO vehicle controls were used at 1% (v/v). Hair follicles were treated with DMSO only as a control. Follicles were imaged typically on day 0 (the day follicles were placed in culture) and again on day 7. The length of the hair fiber was assessed with Vision Builder (National Instruments). The growth of the hair fiber was calculated by subtracting the length on day 0 from that determined on day 7. Each measurement reported is the average of the results from 14 to 20 follicles.

Statistical analysis

For all *P* value calculations, paired Student's *t* test with a one-tailed distribution was calculated and $P < 0.05$ was considered to be significant. All data are means ± SEM. Analysis of variance (ANOVA) test was used to rank genes from microarray as primarily different with respect to site (haired versus bald) and irrespective of person, date of biopsy, or date of microarray. The top 250 genes of the most significant *P* values for this ANOVA analysis were used for further analysis. A paired *t* test was performed on array intensities.

Supplementary Material

Refer to Web version on PubMed Central for supplementary material.

Acknowledgments

We gratefully acknowledge the assistance of J. Tobias and D. Baldwin of the Penn Microarray Facility core, L. Ash in the histology core, and the Penn Human Cooperative Tissue Network.

Funding: NIH grants R01-AR46837, R01-AR055309, P30-AR057217, and K08AR055666; Skin Disease Research Center grant 5-P30-AR-057217-02; Pennsylvania Department of Health; Edwin and Fannie Gray Hall Center for Human Appearance at University of Pennsylvania Medical Center; American Skin Association; Dermatology Foundation; and L'Oreal.

REFERENCES AND NOTES

1. Alsantali A, Shapiro J. Androgens and hair loss. Curr Opin Endocrinol Diabetes Obes. 2009; 16:246–253. [PubMed: 19396986]
2. Richards JB, Yuan X, Geller F, Waterworth D, Bataille V, Glass D, Song K, Waeber G, Vollenweider P, Aben KK, Kiemeney LA, Walters B, Soranzo N, Thorsteinsdottir U, Kong A, Rafnar T, Deloukas P, Sulem P, Stefansson H, Stefansson K, Spector TD, Mooser V. Male-pattern baldness susceptibility locus at 20p11. Nat Genet. 2008; 40:1282–1284. [PubMed: 18849991]
3. Hillmer AM, Hanneken S, Ritzmann S, Becker T, Freudenberg J, Brockschmidt FF, Flaquer A, Freudenberg-Hua Y, Jamra RA, Metzen C, Heyn U, Schweiger N, Betz RC, Blaumeiser B, Hampe J, Schreiber S, Schulze TG, Hennies HC, Schumacher J, Propping P, Ruzicka T, Cichon S, Wienker TF, Kruse R, Nothen MM. Genetic variation in the human androgen receptor gene is the major determinant of common early-onset androgenetic alopecia. Am J Hum Genet. 2005; 77:140–148. [PubMed: 15902657]
4. Paus R, Cotsarelis G. The biology of hair follicles. N Engl J Med. 1999; 341:491–497. [PubMed: 10441606]
5. Oh BR, Kim SJ, Moon JD, Kim HN, Kwon DD, Won YH, Ryu SB, Park YI. Association of benign prostatic hyperplasia with male pattern baldness. Urology. 1998; 51:744–748. [PubMed: 9610587]
6. Price VH. Treatment of hair loss. N Engl J Med. 1999; 341:964–973. [PubMed: 10498493]

7. Messenger AG, Rundegren J. Minoxidil: Mechanisms of action on hair growth. Br J Dermatol. 2004; 150:186–194. [PubMed: 14996087]
8. Lattanand A, Johnson WC. Male pattern alopecia a histopathologic and histochemical study. J Cutan Pathol. 1975; 2:58–70. [PubMed: 777055]
9. Jaworsky C, Kligman AM, Murphy GF. Characterization of inflammatory infiltrates in male pattern alopecia: Implications for pathogenesis. Br J Dermatol. 1992; 127:239–246. [PubMed: 1390168]
10. Cotsarelis G, Sun TT, Lavker RM. Label-retaining cells reside in the bulge area of pilo-sebaceous unit: Implications for follicular stem cells, hair cycle, and skin carcinogenesis. Cell. 1990; 61:1329–1337. [PubMed: 2364430]
11. Garza LA, Yang CC, Zhao T, Blatt HB, Lee M, He H, Stanton DC, Carrasco L, Spiegel JH, Tobias JW, Cotsarelis G. Bald scalp in men with androgenetic alopecia retains hair follicle stem cells but lacks CD200-rich and CD34-positive hair follicle progenitor cells. J Clin Invest. 2011; 121:613–622. [PubMed: 21206086]
12. Colombe L, Michelet JF, Bernard BA. Prostanoid receptors in anagen human hair follicles. Exp Dermatol. 2008; 17:63–72. [PubMed: 18005048]
13. Colombe L, Vindrios A, Michelet JF, Bernard BA. Prostaglandin metabolism in human hair follicle. Exp Dermatol. 2007; 16:762–769. [PubMed: 17697149]
14. Bol DK, Rowley RB, Ho CP, Pilz B, Dell J, Swerdel M, Kiguchi K, Muga S, Klein R, Fischer SM. Cyclooxygenase-2 overexpression in the skin of transgenic mice results in suppression of tumor development. Cancer Res. 2002; 62:2516–2521. [PubMed: 11980643]
15. Johnstone MA, Albert DM. Prostaglandin-induced hair growth. Surv Ophthalmol. 2002; 47(Suppl 1):S185–S202. [PubMed: 12204716]
16. Goodman, LS.; Gilman, A.; Hardman, JG.; Gilman, AG.; Limbird, LE. Goodman & Gilman's the Pharmacological Basis of Therapeutics. 9. McGraw-Hill, Health Professions Division; New York: 1996.
17. Bell-Parikh LC, Ide T, Lawson JA, McNamara P, Reilly M, FitzGerald GA. Biosynthesis of 15-deoxy-$\Delta^{12,14}$-PGJ_2 and the ligation of PPARγ. J Clin Invest. 2003; 112:945–955. [PubMed: 12975479]
18. Müller-Röver S, Handjiski B, van der Veen C, Eichmüller S, Foitzik K, McKay IA, Stenn KS, Paus R. A comprehensive guide for the accurate classification of murine hair follicles in distinct hair cycle stages. J Invest Dermatol. 2001; 117:3–15. [PubMed: 11442744]
19. Hébert JM, Rosenquist T, Götz J, Martin GR. FGF5 as a regulator of the hair growth cycle: Evidence from targeted and spontaneous mutations. Cell. 1994; 78:1017–1025. [PubMed: 7923352]
20. Sasaki S, Hozumi Y, Kondo S. Influence of prostaglandin $F_{2\alpha}$ and its analogues on hair regrowth and follicular melanogenesis in a murine model. Exp Dermatol. 2005; 14:323–328. [PubMed: 15854125]
21. Paus R, Maurer M, Slominski A, Czarnetzki BM. Mast cell involvement in murine hair growth. Dev Biol. 1994; 163:230–240. [PubMed: 8174779]
22. Lyle S, Christofidou-Solomidou M, Liu Y, Elder DE, Albelda S, Cotsarelis G. The C8/144B monoclonal antibody recognizes cytokeratin 15 and defines the location of human hair follicle stem cells. J Cell Sci. 1998; 111(Pt. 21):3179–3188. [PubMed: 9763512]
23. Müller-Decker K, Leder C, Neumann M, Neufang G, Bayerl C, Schweizer J, Marks F, Fürstenberger G. Expression of cyclooxygenase isozymes during morphogenesis and cycling of pelage hair follicles in mouse skin: Precocious onset of the first catagen phase and alopecia upon cyclooxygenase-2 overexpression. J Invest Dermatol. 2003; 121:661–668. [PubMed: 14632179]
24. Muller-Decker K, Neufang G, Berger I, Neumann M, Marks F, Furstenberger G. Transgenic cyclooxygenase-2 overexpression sensitizes mouse skin for carcinogenesis. Proc Natl Acad Sci USA. 2002; 99:12483–12488. [PubMed: 12221288]
25. Matsuoka T, Hirata M, Tanaka H, Takahashi Y, Murata T, Kabashima K, Sugimoto Y, Kobayashi T, Ushikubi F, Aze Y, Eguchi N, Urade Y, Yoshida N, Kimura K, Mizoguchi A, Honda Y, Nagai H, Narumiya S. Prostaglandin D_2 as a mediator of allergic asthma. Science. 2000; 287:2013–2017. [PubMed: 10720327]

26. Satoh T, Moroi R, Aritake K, Urade Y, Kanai Y, Sumi K, Yokozeki H, Hirai H, Nagata K, Hara T, Utsuyama M, Hirokawa K, Sugamura K, Nishioka K, Nakamura M. Prostaglandin D_2 plays an essential role in chronic allergic inflammation of the skin via CRTH2 receptor. J Immunol. 2006; 177:2621–2629. [PubMed: 16888024]
27. Eguchi N, Minami T, Shirafuji N, Kanaoka Y, Tanaka T, Nagata A, Yoshida N, Urade Y, Ito S, Hayaishi O. Lack of tactile pain (allodynia) in lipocalin-type prostaglandin D synthase-deficient mice. Proc Natl Acad Sci USA. 1999; 96:726–730. [PubMed: 9892701]
28. Cossette C, Walsh SE, Kim S, Lee GJ, Lawson JA, Bellone S, Rokach J, Powell WS. Agonist and antagonist effects of 15*R*-prostaglandin (PG) D_2 and 11-methylene-PGD_2 on human eosinophils and basophils. J Pharmacol Exp Ther. 2007; 320:173–179. [PubMed: 17041009]
29. Geng L, Hanson WR, Malkinson FD. Topical or systemic 16,16 Dm prostaglandin E2 or WR-2721 (WR-1065) protects mice from alopecia after fractionated irradiation. Int J Radiat Biol. 1992; 61:533–537. [PubMed: 1349335]
30. Zhu H, Ma H, Ni H, Ma XH, Mills N, Yang ZM. Expression and regulation of lipocalin-type prostaglandin D synthase in rat testis and epididymis. Biol Reprod. 2004; 70:1088–1095. [PubMed: 14668211]
31. Treister NS, Richards SM, Suzuki T, Jensen RV, Sullivan DA. Influence of androgens on gene expression in the BALB/c mouse submandibular gland. J Dent Res. 2005; 84:1187–1192. [PubMed: 16304452]
32. Piprek RP. Genetic mechanisms underlying male sex determination in mammals. J Appl Genet. 2009; 50:347–360. [PubMed: 19875885]
33. Urade Y, Eguchi N. Lipocalin-type and hematopoietic prostaglandin D synthases as a novel example of functional convergence. Prostaglandins Other Lipid Mediat. 2002; 68–69:375–382.
34. Otsuki M, Gao H, Dahlman-Wright K, Ohlsson C, Eguchi N, Urade Y, Gustafsson JA. Specific regulation of lipocalin-type prostaglandin D synthase in mouse heart by estrogen receptorβ. Mol Endocrinol. 2003; 17:1844–1855. [PubMed: 12829806]
35. Ma H, Sprecher HW, Kolattukudy PE. Estrogen-induced production of a peroxisome proliferator-activated receptor (PPAR) ligand in a PPARγ-expressing tissue. J Biol Chem. 1998; 273:30131–30138. [PubMed: 9804768]
36. Amateau SK, McCarthy MM. Induction of PGE2 by estradiol mediates developmental masculinization of sex behavior. Nat Neurosci. 2004; 7:643–650. [PubMed: 15156148]
37. Kvedar JC, Baden HP, Levine L. Selective inhibition by minoxidil of prostacyclin production by cells in culture. Biochem Pharmacol. 1988; 37:867–874. [PubMed: 3278714]
38. Iinuma K, Sato T, Akimoto N, Noguchi N, Sasatsu M, Nishijima S, Kurokawa I, Ito A. Involvement of *Propionibacterium acnes* in the augmentation of lipogenesis in hamster sebaceous glands in vivo and in vitro. J Invest Dermatol. 2009; 129:2113–2119. [PubMed: 19282842]
39. Karnik P, Tekeste Z, McCormick TS, Gilliam AC, Price VH, Cooper KD, Mirmirani P. Hair follicle stem cell-specific *PPAR*γ deletion causes scarring alopecia. J Invest Dermatol. 2009; 129:1243–1257. [PubMed: 19052558]
40. Roman RJ. *P*-450 metabolites of arachidonic acid in the control of cardiovascular function. Physiol Rev. 2002; 82:131–185. [PubMed: 11773611]
41. Jones RL, Giembycz MA, Woodward DF. Prostanoid receptor antagonists: Development strategies and therapeutic applications. Br J Pharmacol. 2009; 158:104–145. [PubMed: 19624532]
42. Norman P. DP_2 receptor antagonists in development. Expert Opin Investig Drugs. 2010; 19:947–961.
43. Li W, Marshall C, Mei L, Dzubow L, Schmults C, Dans M, Seykora J. Srcasm modulates EGF and Src-kinase signaling in keratinocytes. J Biol Chem. 2005; 280:6036–6046. [PubMed: 15579470]
44. Millar SE, Willert K, Salinas PC, Roelink H, Nusse R, Sussman DJ, Barsh GS. WNT signaling in the control of hair growth and structure. Dev Biol. 1999; 207:133–149. [PubMed: 10049570]
45. Philpott MP, Sanders D, Westgate GE, Kealey T. Human hair growth in vitro: A model for the study of hair follicle biology. J Dermatol Sci. 1994; 7:S55–S72. [PubMed: 7999676]

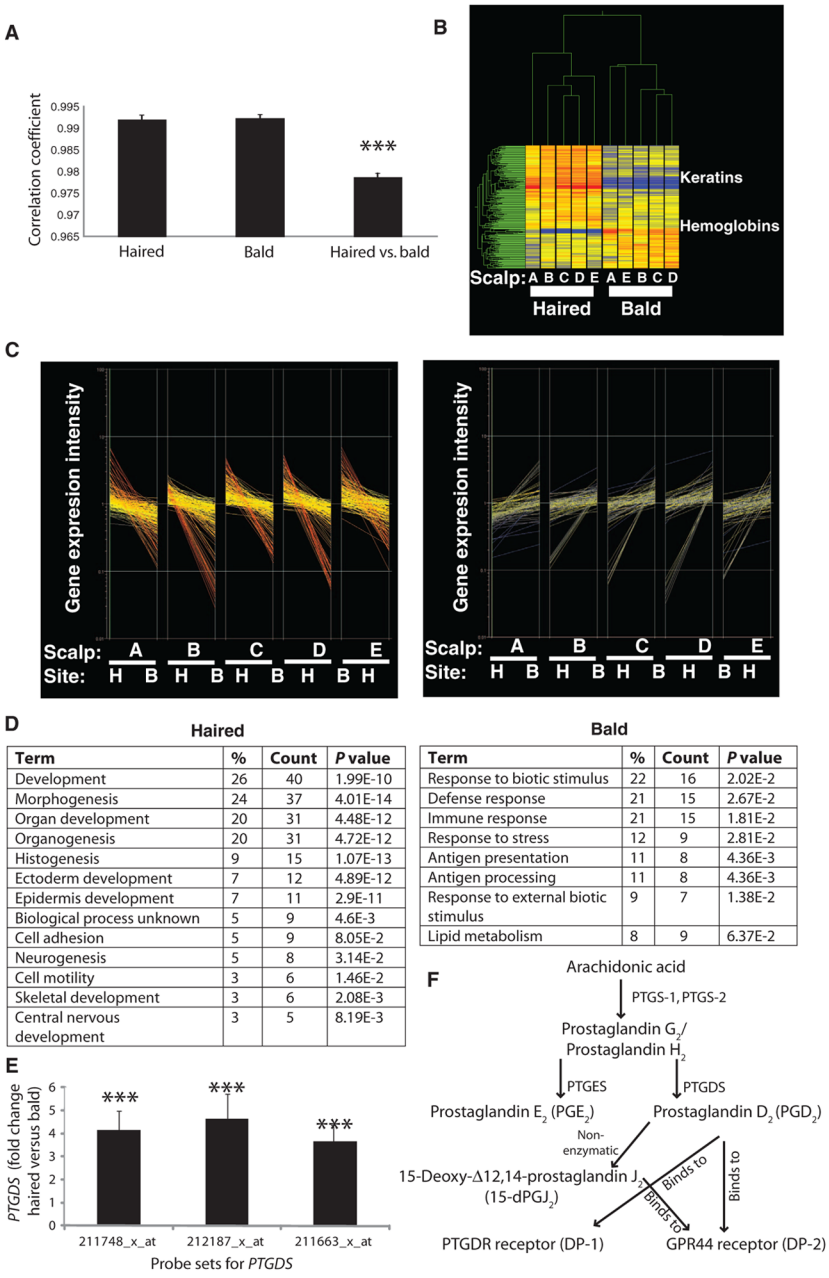

Fig. 1.

Summary of gene expression profiles of haired versus bald scalp from five men with AGA. (**A**) Correlation coefficients to compare the degree of difference between all haired samples, between all bald samples, or between haired versus bald samples within individuals. Data are means ± SEM ($n = 5$). ***$P < 0.001$ compared to both hair only and bald only. (**B**) Gene clustering algorithm of 250 significant genes in haired and bald scalps in five men labeled A to E. (**C**) Discontinuous graphs with gene expression level on the *y* axis and samples grouped as pairs along the *x* axis for the 250 most significant genes divided into those higher in the haired (H) scalp (169; left) and those higher in the bald (B) scalp (81; right). In each pair, the first sample (beginning of line) is the haired scalp and the second sample (end of line) is the bald scalp. (**D**) Gene ontology categories in haired scalp (left) versus balding scalp (right). Percentages listed are numbers of transcripts in each category out of total

number of unique gene transcripts. *P* values are modified Fisher exact EASE (Expression Analysis Systematic Explorer) score for the significant enrichment of each category of function. (**E**) Fold change in *PTGDS* expression in bald scalp compared to haired scalp. Data are means ± SEM ($n = 5$). ***$P < 0.0001$ between haired and bald scalp for each probe set, which covers distinct areas within the *PTGDS* gene. (**F**) Schematic of the PGD_2 pathway.

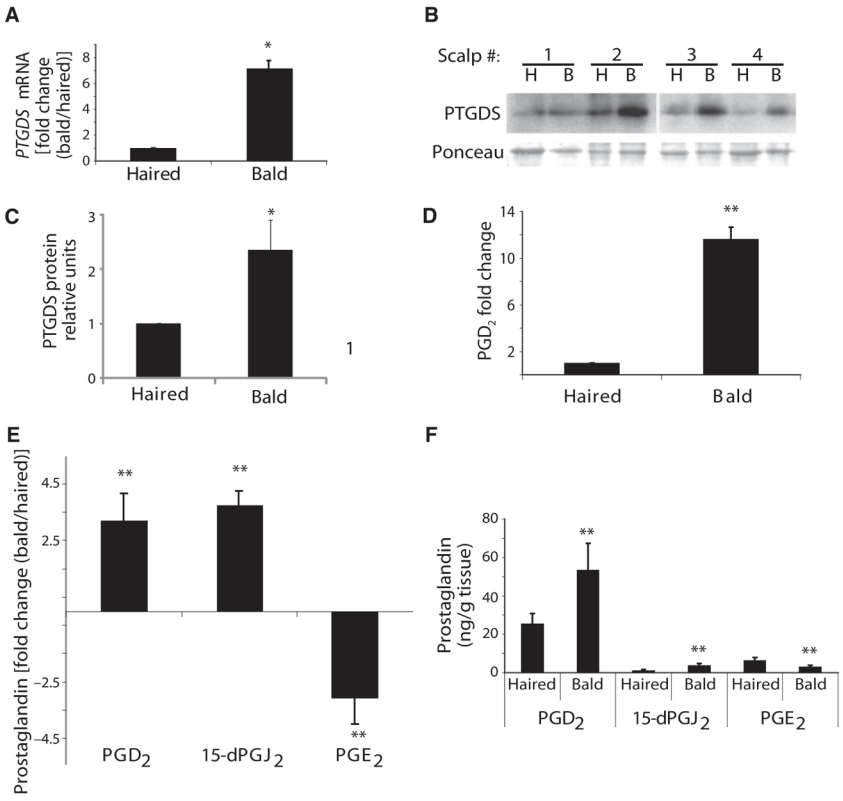

Fig. 2.

Increased PGD_2 pathway activity in balding scalp of men with AGA. (**A**) Expression of lipocalin-type *PTGDS* mRNA in bald versus haired scalp, as tested by qPCR. Data are means ± SEM ($n = 4$). (**B** and **C**) The amount of PTGDS protein in paired bald (B) and haired (H) scalps ($n = 4$), as shown by Western blotting with Ponceau stain used for verification of equal loading (B) and its quantitation as normalized to haired scalp (C). Data are means ± SEM. (**D**) PGD_2 production in bald scalp, as tested by ELISA. Data are means ± SEM ($n = 3$). (**E** and **F**) Fold change in PGD_2 ($n = 17$), 15-$dPGJ_2$) ($n = 7$), and PGE_2 ($n = 17$) expression in bald scalp compared to haired scalp (E). Total prostaglandin content is quantified in (F). Data are means ± SEM. $*P < 0.05$; $**P < 0.01$. In (F), P value compares haired versus bald samples for each prostaglandin.

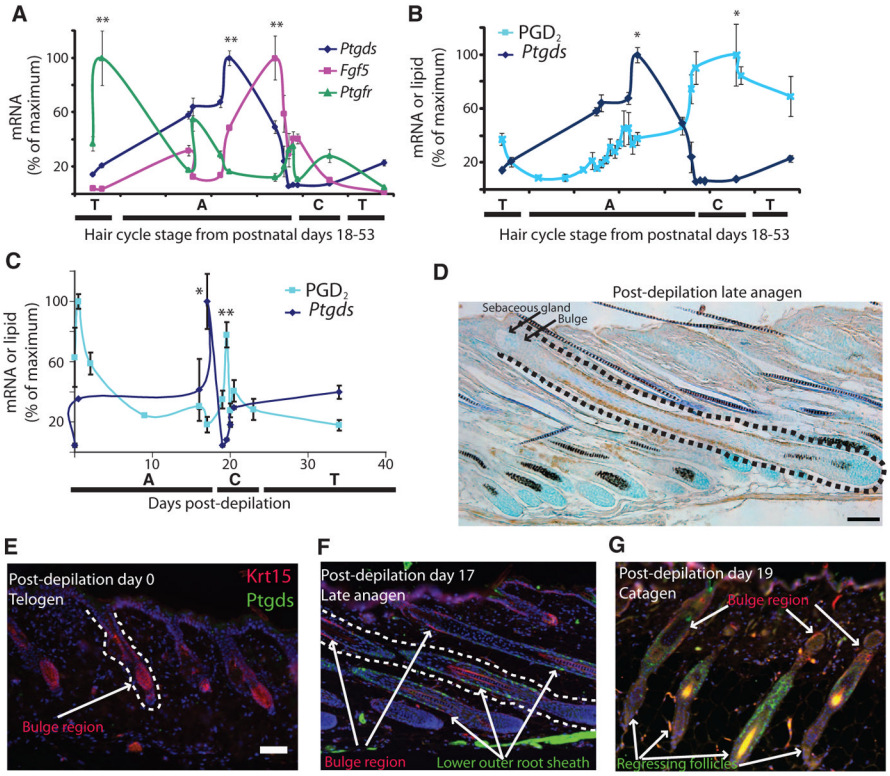

Fig. 3.

An increase in *Ptgds* expression precedes elevation of PGD_2 levels in the murine hair follicle during catagen. (**A** and **B**) At PN18 to PN53, *Ptgds* ($n = 4$), *Ptgfr* ($n = 4$), and *Fgf5* ($n = 4$) mRNA (A and B) and PGD_2 lipid ($n = 3$) (B) were measured at different phases of hair follicle cycling. Letters correspond to hair cycle stages: A, anagen; C, catagen; T, telogen. Data are means ± SEM. In (A), $^{**}P < 0.01$ for *Ptgds* and *Fgf5* late anagen versus first telogen and for *Ptgfr* first telogen versus second telogen. In (B), $^{*}P < 0.05$ for PGD_2 catagen versus early anagen. (**C**) Expression of *Ptgds* ($n = 3$) and production of PGD_2 ($n = 3$) in murine skin during the depilation-induced hair follicle cycle. Data are means ± SEM. $^{*}P < 0.05$ for *Ptgds* on day 17 versus day 0; $^{**}P < 0.01$ for PGD_2 day 19.5 versus day 37. (**D**) Murine outer root sheath keratinocytes below the stem cell–rich bulge area were stained for Ptgds (brown) 17 days after depilation. Dotted line delineates a full hair follicle. Scale bar, 100 μm. (**E** to **G**) Krt15 (red) and Ptgds (green) in permanent and non-permanent compartments of the hair follicle on day 0 (anagen) (E), day 17 (late anagen) (F), and day 19 (catagen) (G) after depilation. Scale bars, 100 μm.

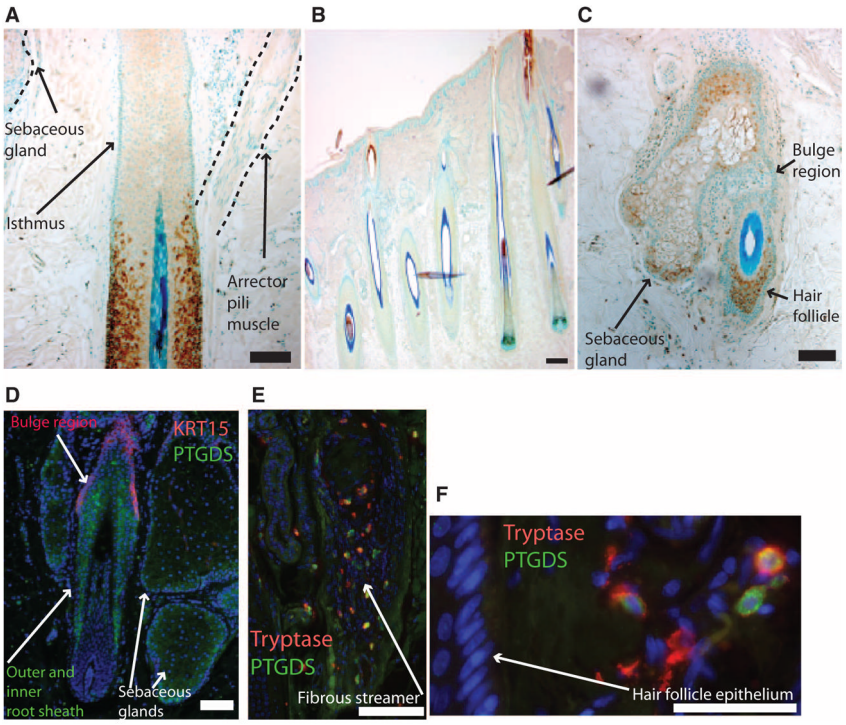

Fig. 4.

PTGDS is expressed in the nonpermanent portion of select human hair follicles in haired scalp, and more variably in bald scalp. (**A** to **C**) PTGDS immunostaining (brown) with blue nuclear counterstain in normal human hair follicles (A and B) and bald scalp hair follicle (C). (A) A single follicle in haired scalp with staining for PTGDS inferior to the isthmus. (B) Most anagen follicles of haired scalp have little staining for PTGDS. (C) Miniaturized hair follicle with PTGDS staining in sebocytes and hair follicle keratinocytes. Scale bars, 100 μm. (**D** to **F**) Immunofluorescence staining for PTGDS (green), nuclei (blue), and either KRT15 (red) (D) or tryptase (red) (E and F) in the hair follicle and adjoining sebaceous gland in bald scalp. Catagen follicle with some PTGDS-positive cells also expressed the mast cell marker tryptase (E). Perifollicular cells show distinct populations of PTGDS- and tryptase-positive cells with overlapping expression (F). Scale bars, 100 μm.

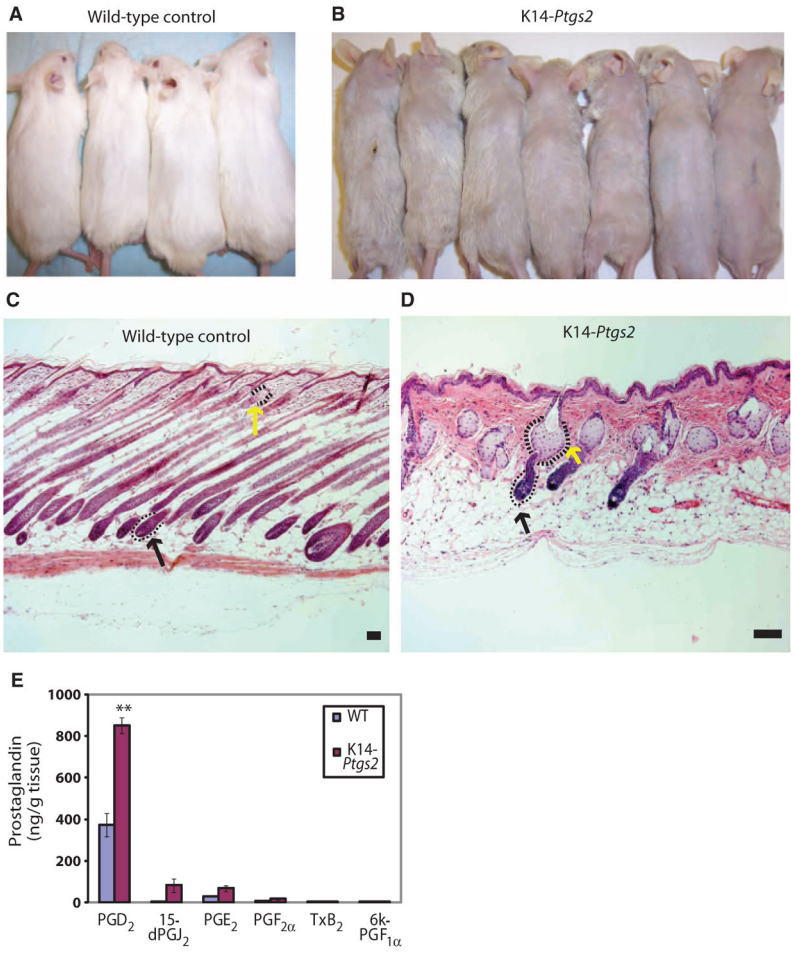

Fig. 5.

K14-*Ptgs2* transgenic mouse skin phenocopies AGA with alopecia, sebaceous gland hyperplasia, and elevated PGD_2 levels in skin. (**A** and **B**) K14-*Ptgs2* animals develop alopecia (B) compared to wild-type (WT) controls (A). (**C** and **D**) Hematoxylin and eosin–stained skin from WT (C) and K14-*Ptgs2* animals (D) shows sebaceous gland (yellow arrow) and hair follicle (black arrow) morphology. Scale bars, 100 μm. (**E**) Amount of different prostaglandins present in skin tissue from WT mice ($n = 5$) and K14-*Ptgs2* transgenic mice ($n = 3$). Data are means ± SEM. $^{**}P < 0.01$ comparing WT to K14-*Ptgs2*.

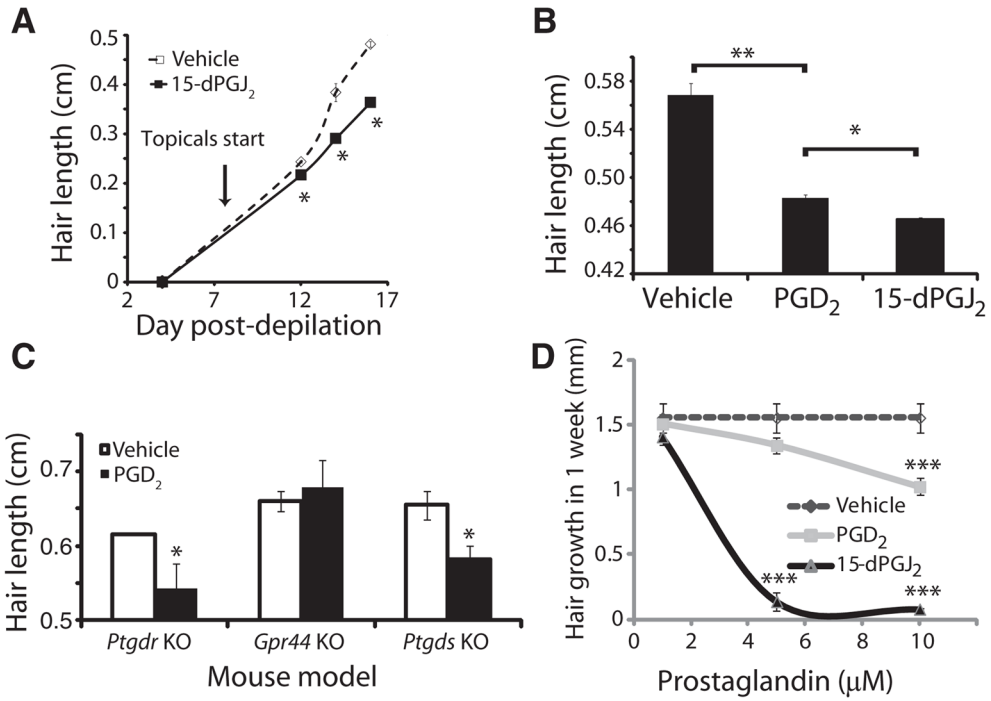

Fig. 6.

PGD_2 inhibits mouse and human hair growth through GPR44. (**A**) Hair growth over the course of 16 days after depilation. 15-$dPGJ_2$ (10 μg) or vehicle was applied topically to mouse skin starting on day 8 after depilation. Data are means ± SEM (n = 3 per treatment group). *P < 0.05 compared to control. (**B**) Hair length 10 days after topical PGD_2 (1 μg; n = 3), 15-$dPGJ_2$ (1 μg; n = 3), or vehicle (n = 3) treatment. Data are means ± SEM. *P < 0.05; **P < 0.01. (**C**) Hair growth in *Ptgdr* (n = 8), *Ptgds* (n = 6), and *Gpr44* (n = 11) knockout (KO) mice in response to PGD_2. Data are means ± SEM and are representative of three independent experiments per mouse. *P < 0.05 compared to vehicle. (**D**) In vitro growth of explanted human hair follicles over the course of 7 days in culture with PGD_2 (n = 3), 15-$dPGJ_2$ (n = 3), or vehicle (n = 3). Data are means ± SEM. ***P < 0.001 compared to vehicle.